

**QED contribution to the color-singlet  $J/\psi$  production in  $Y$  decay near the endpoint**

Xiaohui Liu

*Department of Physics and Astronomy, University of Pittsburgh, Pittsburgh, Pennsylvania 15260, USA*

(Received 4 December 2009; published 19 February 2010)

A recent study indicates that the  $\alpha^2\alpha_s^2$  order QED processes of  $Y \rightarrow J/\psi + X$  decay are compatible with those of QCD processes. However, in the endpoint region, the nonrelativistic QED calculation breaks down since the collinear degrees of freedom are missing under the framework of this effective theory. In this paper we apply the soft-collinear effective theory (SCET) to study the color-singlet QED process at the kinematic limit. Within this approach we are able to sum the kinematic logarithms by running operators using the renormalization group equations of soft-collinear effective theory, which will lead to a dramatic change in the momentum distribution near the endpoint and the spectrum shape consistent with the experimental results.

DOI: 10.1103/PhysRevD.81.034027

PACS numbers: 13.60.Le, 14.40.Lb, 14.40.Pq

**I. INTRODUCTION**

During the past 15 years, the interactions of nonrelativistic heavy quarks inside quarkonium have been understood to some extent using the framework of nonrelativistic effective theories [1,2]. These theories reproduce the physics of full QCD or QED by adding local interactions that systematically incorporate relativistic corrections through any given order in the heavy quark velocity  $v$ . They provide generalized factorization theorems that include nonperturbative corrections to the color-singlet model, including color-octet decay mechanisms. All infrared divergences can be factored into nonperturbative matrix elements, so that infrared safe calculations of inclusive decay rates are possible [3]. These nonrelativistic effective theories solve some important phenomenological problems in quarkonium physics. For instance, they provide the most convincing explanation to the surplus  $J/\psi$  and  $\psi'$  production at the Tevatron [4], in which a gluon fragments into a color-octet  $c\bar{c}$  pair in a pointlike color-octet S-wave state which evolves nonperturbatively into the charmonium states plus light hadrons. The factorization formalism allows these fragmentation procedures to be factored into the product of short distance coefficients and long distance matrix elements among which the leading one is  $\langle \mathcal{O}_{\psi(\psi')}^8[{}^3S_1] \rangle$  where  $\mathcal{O}_{\psi(\psi')}^8$  are local four-fermion operators in terms of the nonrelativistic fields.

There are, however, some problems that remain to be solved. One challenging problem is with the polarization of  $J/\psi$  at the Tevatron. The same mechanism that produces the  $J/\psi$  described above predicts the  $J/\psi$  should become transversely polarized as the transverse momentum  $p_\perp$  becomes much larger than  $2m_c$  [5]. Though the theoretical prediction is consistent with the experimental data at intermediate  $p_\perp$ , at the largest measured values of  $p_\perp$  the  $J/\psi$  is observed to be slightly longitudinally polarized and discrepancies at the  $3\sigma$  level are seen in both prompt  $J/\psi$  and  $\psi'$  polarization measurements [6].

A new problem arose as a result of measurements of the spectrum of  $J/\psi$  produced in the  $Y(1S)$  decay by the CLEO III detector at the Cornell Electron Storage Ring (CESR) [7]. Nonrelativistic QCD (NRQCD) calculations have been made for the production of  $J/\psi$  through both color-singlet and color-octet configurations [8,9]. Theoretical calculations predict that the color-singlet process  $Y(1S) \rightarrow J/\psi c\bar{c}g + X$  features a soft momentum spectrum. Meanwhile, the theoretical estimates based on color-octet contributions indicate that the momentum spectrum peaks near the kinematic endpoint [9]. In contrast to the theoretical predictions, the experimentally measured momentum spectrum is significantly softer than predicted by the color-octet model and somewhat softer than the color-singlet case [7].

A more detailed study on the color-singlet contribution to this process has been presented recently [10]. It was found that the contribution of the color-singlet QED process is comparable with the QCD process. Nonrelativistic QED (NRQED) calculations indicate that the QED process will give a large contribution to the spectrum near the endpoint that is not observed in the data. This contribution results from the  $J/\psi$  being produced back-to-back with a pair of gluons forming a low-mass jet. However, in this region of phase space, the NRQED calculation breaks down, since it does not contain the correct degrees of freedom. NRQED contains soft quarks, photons, and gluons, but it does not contain quarks and gluons moving collinearly. The correct effective theory to use in situations where there is both soft and collinear physics is soft-collinear effective theory (SCET) [11–14].

A similar situation happens when studying  $e^+e^- \rightarrow J/\psi + X$ . The combination of SCET and NRQCD has been successful in reproducing the shape of the measured  $J/\psi$  momentum spectrum in  $e^+e^- \rightarrow J/\psi + X$  [15]. SCET has the power to describe the endpoint regime by including the light energetic degrees of freedom. In addition, the renormalization group equations of SCET can be

used to resum large perturbative logarithmic corrections. The nonperturbative NRQCD matrix elements arise naturally in deriving the factorization theorem using SCET.

In this paper, we use SCET to study the color-singlet contribution to the  $Y \rightarrow J/\psi + X$  decay near the endpoint via a virtual photon. We derive the factorization theorem in SCET for this process. We find that the spectrum is softer than the tree order prediction of NRQED when including perturbative and nonperturbative corrections near the endpoint, giving better agreement with the data than the previous predictions.

## II. MATCHING AND FACTORIZATION

In this section, we derive the SCET factorization theorem for the color-singlet contribution to  $Y \rightarrow J/\psi + X$  via a virtual photon near the endpoint. This factorization formula is crucial since the NRQED does not properly include the relevant collinear degrees of freedom and thus breaks down in this regime. This can be understood by analyzing the kinematics near the endpoint. In the center-of-mass frame, we have

$$\begin{aligned} p_Y^\mu &= \frac{M_Y}{2} n^\mu + \frac{M_Y}{2} \bar{n}^\mu + k_Y^\mu, \\ p_\psi^\mu &= \frac{M_\psi^2}{2zM_Y} n^\mu + \frac{zM_Y}{2} \bar{n}^\mu + k_\psi^\mu, \\ p_X^\mu &= \frac{M_Y}{2} \left[ \left(1 - \frac{r}{z}\right) n^\mu + (1-z) \bar{n}^\mu \right] + k_X^\mu. \end{aligned} \quad (1)$$

Here  $n = (1, 0, 0, 1)$  and  $\bar{n} = (1, 0, 0, -1)$ , we have defined  $z = (E_\psi + p_\psi)/M_Y$  and  $r = m_c^2/m_b^2$ . We also assumed that  $M_\psi = 2m_c$  and  $M_Y = 2m_b$ .  $k_Y^\mu$  and  $k_\psi^\mu$  are the residual momentum of the  $Q\bar{Q}$  pair inside the  $Y$  and  $J/\psi$  respectively. Near the kinematic endpoint, the variable  $z \rightarrow 1$  and thus the jet invariant mass approaches zero. In NRQED, an expansion of  $k^\mu/m_X$  is performed and hence the jet mode is integrated out, which is only valid when the jet mass is large compare to the residual momentum. The invariant mass of the jet is large away from the endpoint. As  $z \rightarrow 1$ , the jet becomes energetic, with small invariant mass. Hence we must keep  $k^\mu/m_X$  to all orders. As a result, the standard NRQED factorization breaks down at the endpoint. SCET is the appropriate framework for properly including the collinear modes needed in the endpoint in order to make reasonable predictions.

To derive the factorization theorem in SCET, we start with the optical theorem in which the decay rate is written as

$$\begin{aligned} 2E_\psi \frac{d\Gamma}{d^3p_\psi} &= \frac{1}{32\pi^3 m_b} \sum_X \int d^4y e^{-iq \cdot y} \langle Y | \mathcal{O}^\dagger(y) | J/\psi + X \rangle \\ &\quad \times \langle J/\psi + X | \mathcal{O}(0) | Y \rangle, \end{aligned} \quad (2)$$

where the summation includes integration over the  $X$  phase space, which includes both the ultrasoft (usoft)  $X_u$  and collinear  $X_c$  sectors. The SCET operator  $\mathcal{O}$  is of the form

$$\mathcal{O} = \sum_\omega e^{-i(M_Y v + \bar{P}(n/2)) \cdot y} C(\mu, \omega) \Gamma_{\alpha\beta\mu\nu} \mathcal{J}^{\alpha\beta}(\omega) \mathcal{O}_{J/\psi}^\mu \mathcal{O}_Y^\nu, \quad (3)$$

where the Wilson coefficient  $C(\mu, \omega)$  is obtained by matching from QCD to SCET at some hard scale  $\mu = \mu_H$ . The operator is constrained by the gauge invariance. In our case, to leading order we have

$$\mathcal{J}^{\alpha\beta}(\omega) = \text{Tr}[B_{\perp\omega_1}^\alpha B_{\perp\omega_2}^\beta], \quad (4)$$

$$\mathcal{O}_{J/\psi}^\mu = \psi_c^\dagger (\Lambda_1 \cdot \sigma)^\mu \chi_c, \quad (5)$$

$$\mathcal{O}_Y^\nu = \chi_b^\dagger (\Lambda_2 \cdot \sigma)^\nu \psi_b. \quad (6)$$

Here the  $\Lambda$ 's boost the  $J/\psi$  or  $Y$  from the center-of-mass frame to an arbitrary frame.  $\psi$  and  $\chi$  are the heavy quark and antiquark fields which create or annihilate the constituent heavy (anti)quarks inside the quarkonia. The collinear gauge invariant field strength  $B_\perp^\alpha$  is built out of the collinear gauge field  $A_{n,q}^\alpha$

$$B_\perp^\alpha = \frac{-i}{g_s} W_n^\dagger (\mathcal{P}_\perp^\alpha + g_s (A_{n,q}^\alpha)_\perp) W_n, \quad (7)$$

where

$$W_n = \sum_{\text{perms}} \exp\left(-g_s \frac{1}{\bar{P}} \bar{n} \cdot A_{n,q}\right) \quad (8)$$

is the collinear Wilson line. The operator  $\mathcal{P}$  is used to project out the large momentum label [13].

The hard coefficient containing the spin structure is obtained by matching the Feynman diagrams shown in Fig. 1, which gives

$$\Gamma_{\alpha\beta\mu\nu} = i \frac{32\pi^2}{2N_c} \frac{e_c e_b \alpha \alpha_s}{m_c m_b} g_{\alpha\beta}^\perp g_{\mu\nu}^\perp, \quad (9)$$

where  $g_{\mu\nu}^\perp = g_{\mu\nu} - (n_\mu \bar{n}_\nu + n_\nu \bar{n}_\mu)/2$ . We have chosen the hard coefficient so that the Wilson coefficient  $C(\mu, \omega)$  is 1 at the hard scale  $\mu_H$ .

Inserting the operator in Eq. (3) into Eq. (2),  $\mathcal{O}^\dagger(y)$  picks an additional phase, and the differential rate becomes

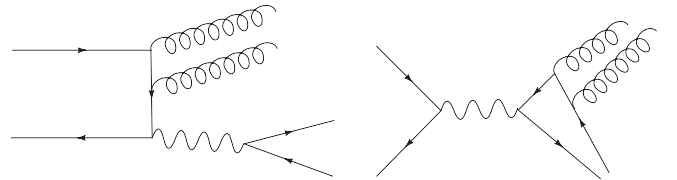


FIG. 1. Diagrams for the QED contribution to the color-singlet  $J/\psi$  production via  $Y$  decay at order  $\alpha^2 \alpha_s^2$ .

$$\begin{aligned}
 2E_\psi \frac{d\Gamma}{d^3 p_\psi} &= \frac{1}{32\pi^3 m_b} \sum_X \sum_{\omega\omega'} C^\dagger(\mu, \omega) C(\mu, \omega') \int d^4 y e^{-iM_Y/2(1-z)\bar{n}\cdot y} \Gamma_{\alpha\beta\mu\nu}^\dagger \Gamma_{\alpha'\beta'\mu'\nu'} \langle Y | \mathcal{J}_\omega^{\alpha\beta\dagger} \mathcal{O}_{J/\psi}^{\mu\dagger} \mathcal{O}_Y^{\nu\dagger}(y) | J/\psi + X \rangle \\
 &\quad \times \langle J/\psi + X | \mathcal{J}_{\omega'}^{\alpha'\beta'} \mathcal{O}_{J/\psi}^{\mu'} \mathcal{O}_Y^{\nu'}(0) | Y \rangle \\
 &\equiv \sum_{\omega\omega'} C^\dagger(\mu, \omega) C(\mu, \omega') \Gamma_{\alpha\beta\mu\nu}^\dagger \Gamma_{\alpha'\beta'\mu'\nu'} \mathcal{A}_{\omega\omega'}^{\alpha\beta\mu\nu, \alpha'\beta'\mu'\nu'}.
 \end{aligned} \tag{10}$$

In the exponent of Eq. (10), we have used  $q^\mu - M_Y v^\mu + \bar{\mathcal{P}} n^\mu / 2 \approx M_Y / 2 (1 - z) \bar{n}^\mu$ . Furthermore, we can decouple the usoft modes from the collinear degrees of freedom using the field redefinition [14]

$$A_{n,q}^\mu = Y A_{n,q}^{(0)\mu} Y^\dagger. \tag{11}$$

The fields with the superscript (0) do not interact with usoft degrees of freedom. In the color-singlet contribution the usoft Wilson lines  $Y$  cancel since  $Y^\dagger Y = 1$ . The  $Y$  and the  $J/\psi$  states contain no collinear quanta, so we can write

$$\mathcal{A}_{\omega\omega'}^{\alpha\beta\mu\nu, \alpha'\beta'\mu'\nu'} = \frac{1}{32\pi^3 m_b} \int d^4 y e^{-iM_Y/2(1-z)\bar{n}\cdot y} \langle Y | \mathcal{O}_{J/\psi}^{\mu\dagger} \mathcal{O}_Y^{\nu\dagger}(y) a_\psi^\dagger a_\psi \mathcal{O}_{J/\psi}^{\mu'} \mathcal{O}_Y^{\nu'}(0) | Y \rangle \langle 0 | \mathcal{J}_\omega^{\alpha\beta\dagger}(y) \mathcal{J}_{\omega'}^{\alpha'\beta'}(0) | 0 \rangle. \tag{12}$$

Here we defined an interpolating field  $a_\psi$  for the  $J/\psi$  and used the completeness of states in the usoft and collinear fields

$$\sum_{X_u} |J/\psi + X_u\rangle \langle J/\psi + X_u| = |J/\psi\rangle \langle J/\psi| \equiv a_\psi^\dagger a_\psi, \tag{13}$$

$$\sum_{X_c} |X_c\rangle \langle X_c| = 1. \tag{14}$$

The  $Y$  is a very compact bound state, due to the large  $b$ -quark mass. In a multipole expansion, long wavelength gluons interact with the  $Y$  color charge distribution through its color dipole moment since the state itself is color neutral. In the theoretical limit of very heavy bottom quark, this coupling to the dipole vanishes [16]. Therefore we are able to write

$$\mathcal{A}_{\omega\omega'}^{\alpha\beta\mu\nu, \alpha'\beta'\mu'\nu'} = \frac{1}{32\pi^3 m_b} \int d^4 y e^{-iM_Y/2(1-z)\bar{n}\cdot y} \langle Y | \mathcal{O}_Y^{\nu\dagger}(y) \mathcal{O}_Y^{\nu'}(0) | Y \rangle \langle 0 | \mathcal{O}_{J/\psi}^{\mu\dagger}(y) a_\psi^\dagger a_\psi \mathcal{O}_{J/\psi}^{\mu'}(0) | 0 \rangle \langle 0 | \mathcal{J}_\omega^{\alpha\beta\dagger}(y) \mathcal{J}_{\omega'}^{\alpha'\beta'}(0) | 0 \rangle. \tag{15}$$

To proceed, we introduce the shape function for  $J/\psi$

$$S_\psi(l^+) = \int \frac{dy^-}{4\pi} e^{-(i/2)l^+ y^-} \frac{\langle 0 | [\chi_{\bar{c}}^\dagger \sigma_i \psi_c(y^-) a_\psi^\dagger a_\psi \psi_{\bar{c}}^\dagger \sigma_i \chi_{\bar{c}}] | 0 \rangle}{4m_c \langle \mathcal{O}_\psi^1 [^3S_1] \rangle}, \tag{16}$$

as well as the shape function for  $Y$

$$S_Y(l^+) = \int \frac{dy^-}{4\pi} e^{-(i/2)l^+ y^-} \frac{\langle Y | \chi_{\bar{b}}^\dagger \sigma_i \psi_b(y^-) \psi_{\bar{b}}^\dagger \sigma_i \chi_{\bar{b}} | Y \rangle}{4m_b \langle Y | \mathcal{O}_Y^1 [^3S_1] | Y \rangle}. \tag{17}$$

Both shape functions are normalized so that  $\int dl^+ S_{\psi, Y}(l^+) = 1$ . The color-singlet shape functions can be related simply to the color-singlet NRQCD matrix elements [17],

$$\langle \chi^\dagger \sigma_i \psi \delta(in \cdot \partial - k^+) \psi^\dagger \sigma_i \chi \rangle = \Theta(k^+) \langle \chi^\dagger \sigma_i \psi \psi^\dagger \sigma_i \chi \rangle, \tag{18}$$

which amounts to a shift from the partonic to hadronic endpoint.

In addition a jet function  $J_\omega(k^+)$  is defined as

$$\langle 0 | \text{Tr}[B_\alpha^\perp B_\beta^\perp](y) \text{Tr}[B_{\alpha'}^\perp B_{\beta'}^\perp](0) | 0 \rangle = i \frac{N_c^2 - 1}{2} (g_{\alpha\alpha'} g_{\beta\beta'} + g_{\alpha\beta'} g_{\beta\alpha'}) \delta_{\omega\omega'} \int \frac{dk^+}{2\pi} \delta^{(2)}(y^\perp) \delta(y^+) e^{-(i/2)k^+ y^-} J_\omega(k^+). \tag{19}$$

The leading-order result for the collinear jet function is [18]

$$J_\omega(k^+) = \frac{1}{8\pi} \Theta(k^+) \int_0^1 d\xi \delta_{\xi, (M_Y + \omega)/(2M_Y)}. \quad (20)$$

Using the spin symmetry relation [19]

$$\Lambda_i^\delta \Lambda_j^{\delta'} \langle \dots \sigma^i \dots \sigma^j \dots \rangle = \frac{1}{3} \delta^{ij} \Lambda_i^\delta \Lambda_j^{\delta'} \langle \dots \sigma^k \dots \sigma^k \dots \rangle, \quad (21)$$

and applying the identity  $\delta^{ij} \Lambda_i^\delta \Lambda_j^{\delta'} = (v^\delta v^{\delta'} - g^{\delta\delta'})$ , where  $v^\delta$  is the four-velocity of the  $Y$  or  $J/\psi$ , we can write the decay rate as

$$\frac{d\Gamma}{dp_\psi} = \Gamma_0 P[x, r] \int_{-1}^1 \frac{d\xi}{2} |C(M_Y \xi, \mu)|^2 \Theta(M_Y - 2E_X), \quad (22)$$

in which

$$\Gamma_0 = \frac{4\pi}{9} \frac{N_c^2 - 1}{N_c^2} \frac{e_b^2 e_c^2 \alpha^2 \alpha_s^2}{m_b^3 m_c^3} \frac{(1-r)^2}{1+r} \langle Y | \mathcal{O}_Y^1[{}^3S_1] | Y \rangle \times \langle \mathcal{O}_\psi^1[{}^3S_1] \rangle, \quad (23)$$

and  $P[x, r] = (x^2 - 4r)(1+r)/(x(1-r)^2)$ . Near the endpoint,  $P[x, r] \rightarrow 1$ . The variable  $x$  is defined as  $x = E_\psi/m_b$ . It is straight forward to check that to the leading order the differential decay rate reproduces the NRQED calculation [10].

### III. RESUMMING SUDAKOV LOGARITHMS AND PHENOMENOLOGY

SCET has the power to sum logarithms using the renormalization group equations (RGEs). Large logarithms arise naturally in the processes involving several well-separated scales and will cause the perturbative expansion breaking down. By matching onto an effective theory, the large scale is removed and replaced by a running scale  $\mu$ . After matching at the high scale, the operators are run to the low scale using the RGEs. This sums all large logarithms into an overall factor, and any logarithms that arise in the perturbative expansion of the effective theory are of order one.

In the previous section, we have matched onto the SCET color-singlet operator, by integrating out the large scale  $\mu_H$ , replacing it with a running scale  $\mu$ . We now run the operator from the hard scale to the collinear scale, which sums all logarithms. The counterterm as well as the anomalous dimension used for running the operator in the RGEs have already been calculated in Ref. [18], and we can lift the results from that paper. The result for the resummed differential decay rate is given by

$$\frac{1}{\Gamma_0} \frac{d\Gamma_{\text{resum}}}{dp_\psi} = P[x, r] \Theta(M_Y - 2E_X) \int d\eta \left[ \frac{\alpha_s(\mu_c)}{\alpha_s(\mu_H)} \right]^{2\gamma(\eta)}, \quad (24)$$

where  $\gamma$  is defined as

$$\gamma \equiv \frac{2}{\beta_0} \left[ C_A \left( \frac{11}{6} + (\eta^2 + (1-\eta)^2) \times \left( \frac{1}{1-\eta} \ln \eta + \frac{1}{\eta} \ln(1-\eta) \right) \right) - \frac{n_f}{3} \right]. \quad (25)$$

To sum the large logarithms, the collinear scale  $\mu_c^2$  is chosen to be approximately  $m_X^2$  and the hard scale is set to be  $\mu_H = 2m_c$ , in same way as in Ref. [10].

The result from Eq. (24) sums up the leading logarithmic corrections which are important only near the endpoint. Away from the endpoint, the logarithms that we have summed are not important and contributions that we neglected in the endpoint become dominant. We therefore would like to interpolate between the leading-order NRQED color-singlet calculation away from the endpoint and the resummed result in the endpoint. To do this, we define the interpolated differential rate as

$$\frac{1}{\Gamma_0} \frac{d\Gamma}{dp_\psi} = \left( \frac{1}{\Gamma_0} \frac{d\Gamma_{\text{LO}}^{\text{dir}}}{dp_\psi} - P[x, r] \right) + \frac{1}{\Gamma_0} \frac{d\Gamma_{\text{resum}}}{dp_\psi}. \quad (26)$$

The first term in parentheses vanishes when approaching the kinematic limit, leaving only the resummed contribution in that region. Away from the endpoint the resummed contribution combines with the  $-P[x, r]$  to give higher order corrections in  $\alpha_s(\mu_H)$  to the spectrum.

In Fig. 2, we compare the resummed, interpolated decay rate, Eq. (26), to the leading-order color-singlet result [10]. We use  $m_c = 1.548$  GeV and  $m_b = 4.73$  GeV.  $\Lambda_{\text{QCD}}$  is set to 0.21 GeV so that  $\alpha_s(2m_c) = 0.259$ . In our figure, the

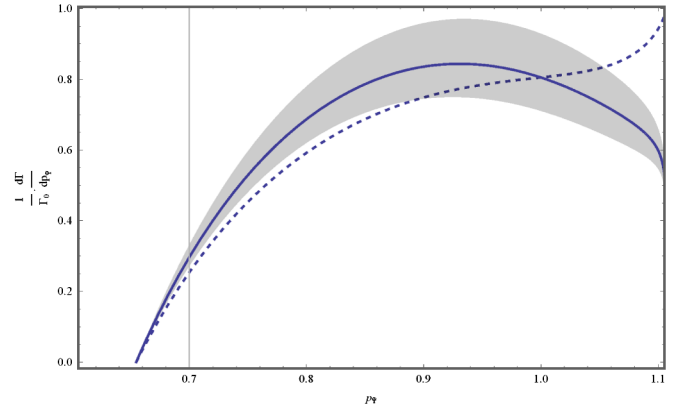


FIG. 2 (color online). The decay rate  $1/\Gamma_0 d\Gamma/dp_\psi$  via QED process. The dashed curve is the tree level direct rate [10]. The solid line presents the interpolated resummed direct rate. The shaded band is obtained by varying the collinear scale from  $\mu_c = m_X/\sqrt{2}$  to  $\mu_c = \sqrt{2}m_X$ , since the choice of scale could only be determined by a higher order calculation.

dashed line presents the leading-order color-singlet calculation and the solid curve corresponds to the interpolated decay rate with the collinear scale chosen as  $\mu_c = m_X$ . The shaded band is obtained by varying the collinear scale from  $\mu_c = m_X/\sqrt{2}$  to  $\mu_c = \sqrt{2}m_X$ , since the choice of scale could only be determined by higher order corrections. After resumming the spectrum shape softens near the endpoint and is thus more consistent with experimental data [7].

#### IV. CONCLUSION

In this work, we study the color-singlet QED process for  $J/\psi$  production in  $Y$  decay in the kinematic limit region. Since the NRQED breaks down at this limit, we apply the SCET to study the spectrum. Our calculation consists of matching onto a color-singlet operator in SCET by integrating out the hard scale. Once the usoft modes are decoupled from the collinear modes using a field redefinition, we are able to show a factorization theorem for the

differential decay rate, in which the decay rate can be factorized into a hard piece, a collinear jet function, and usoft functions. As pointed out by Ref. [17] the usoft function in this case can be calculated, resulting in just a shift from the partonic to the physical endpoint.

By running the resulting rate from the hard scale  $\mu_H$  to the collinear scale  $\mu_c$ , we sum the large Sudakov logarithms. Finally, we combine the SCET calculation with the leading-order, color-singlet NRQED result to make a prediction for the color-singlet contribution via QED process to the differential decay rate spectrum over the entire allowed kinematic range.

#### ACKNOWLEDGMENTS

I would like to thank Professor A. K. Leibovich for guidances and carefully reading the manuscript and checking all the calculations. X. L. was supported in part by the National Science Foundation under Grant No. PHY-0546143.

- 
- [1] G. T. Bodwin, E. Braaten, and G. P. Lepage, Phys. Rev. D **51**, 1125 (1995).  
 [2] M. E. Luke, A. V. Manohar, and I. Z. Rothstein, Phys. Rev. D **61**, 074025 (2000).  
 [3] G. T. Bodwin, E. Braaten, and G. P. Lepage, Phys. Rev. D **46**, R1914 (1992).  
 [4] E. Braaten and S. Fleming, Phys. Rev. Lett. **74**, 3327 (1995).  
 [5] P. L. Cho and M. B. Wise, Phys. Lett. B **346**, 129 (1995); A. K. Leibovich, Phys. Rev. D **56**, 4412 (1997); M. Beneke and M. Kramer, Phys. Rev. D **55**, R5269 (1997); E. Braaten, B. A. Kniehl, and J. Lee, Phys. Rev. D **62**, 094005 (2000).  
 [6] T. Affolder *et al.* (CDF Collaboration), Phys. Rev. Lett. **85**, 2886 (2000).  
 [7] R. A. Briere *et al.* (CLEO Collaboration) Phys. Rev. D **70**, 072001 (2004).  
 [8] Shi-yuan Li, Qu-bing Xie, and Qun Wang, Phys. Lett. B **482**, 65 (2000).  
 [9] Kingman Cheung, Wai-Yee Keung, and Tzu Chiang Yuan, Phys. Rev. D **54**, 929 (1996).  
 [10] Zhi-Guo He and Jian-Xiong Wang, arXiv:0911.0139.  
 [11] C. W. Bauer, S. Fleming, and M. Luke, Phys. Rev. D **63**, 014006 (2000).  
 [12] C. W. Bauer, S. Fleming, D. Pirjol, and I. W. Stewart, Phys. Rev. D **63**, 114020 (2001).  
 [13] C. W. Bauer and I. W. Stewart, Phys. Lett. B **516**, 134 (2001).  
 [14] C. W. Bauer, D. Pirjol, and I. W. Stewart, Phys. Rev. D **65**, 054022 (2002).  
 [15] S. Fleming, A. K. Leibovich, and T. Mehen, Phys. Rev. D **68**, 094011 (2003).  
 [16] C. Bobeth, B. Grinstein, and M. Savrov, Phys. Rev. D **77**, 074007 (2008).  
 [17] I. Z. Rothstein and M. B. Wise, Phys. Lett. B **402**, 346 (1997); M. Beneke, I. Z. Rothstein, and M. B. Wise, Phys. Lett. B **408**, 373 (1997).  
 [18] S. Fleming and A. K. Leibovich, Phys. Rev. D **67**, 074035 (2003).  
 [19] E. Braaten and Y. Q. Chen, Phys. Rev. D **54**, 3216 (1996).